

# Pulsed Picosecond and Nanosecond Discharge Development in Liquids with Various Dielectric Permittivity Constants

Andrey Starikovskiy<sup>1</sup>

<sup>1</sup>*Princeton University, Mechanical and Aerospace Department, Princeton, 08544 NJ, USA*

The dynamics of pulsed picosecond and nanosecond discharge development in liquid water, ethanol and hexane were investigated experimentally. It is shown that the dynamics of discharge formation fundamentally differ between liquids with low and high dielectric permittivity coefficients. The difference in the nanosecond discharge development in liquid dielectrics may be explained by the formation of micro-discontinuities in the media during the electrostriction compression/rarefaction stage in liquids with high dielectric permittivities.

## Introduction

Discharge processes in liquids have been of interest for a long time, beginning with the analysis of electrical insulation properties in different systems [1]. Recently, the range of possible applications for discharges in liquids was extended to the areas of water sterilization [2], bio-medical applications [3], and water quality control [4].

New applications require excitation of the liquid with a minimal temperature increase. The simplest solution to the problem is the high-voltage pulse length decrease [5]. High-voltage pulses of picosecond duration allow the maintenance of an extremely high electrical field in the plasma formation region, comparable to the intra-molecular field. In the super-strong fields, ionization in the condensed phase can be achieved by direct electron impact [5]. At the sub-nanosecond time scale, the fluid lacks time to expand; hence, the density of matter remains close to the initial value, and the discharge is formed directly in the liquid phase without undergoing a phase transition [5].

In contrast, under microsecond discharge conditions, sufficient time for the hydrodynamic expansion of a liquid always exists because of the strong electrostatic repulsion of the charged walls of the channels [1]. As such, the discharge usually develops in the low density channels.

The intermediate case for discharge development is discharge on a nanosecond time scale [6]. In this range, the time of hydrodynamic expansion is sufficiently long in comparison to the time of discharge; however, expansion allows for the formation of microscopic voids within the liquid in the region of the strong fields, resulting from electrostriction forces [7].

A strong electric field appears in the dielectric fluid near the tip of the high-voltage electrode. The field

gradient leads to the formation of a strong pressure gradient, which is directed along the electric field lines. If the voltage rise time is in the range of a few nanoseconds, this time apparently is sufficient to cause displacement of the fluid particles on the order of a few molecular layers [7]. Such a shift should form nanoscale discontinuities in the continuous medium, where the electrons gain energy significantly more quickly than in the condensed phase. This mechanism can provide an effective starting point for discharge from the electrode. It should be noted that the mechanism [7] cannot explain the subsequent maintenance of the conduction channel over a long time scale, because the electric field decrease in the channel of the streamer inevitably leads to pressure redistribution and the collapse of the microscopic voids formed during the first phase of discharge. The conductivity of a dielectric liquid in a relatively weak field is insufficient for electric potential propagation from the high-voltage electrode, causing the discharge development to cease. However, on a longer time scale, the mechanism of low-density channel maintenance can switch from electrostriction to an electrostatic mechanism; on a time scale 10-100 ns, this change can provide sufficient expansion velocity of the conductive low-density channels.

A long pulse (microsecond scale) scenario has been investigated previously, with the details given in the literature [1]. The dynamics of plasma channel formation at a velocity of up to 15% of the local speed of light in a liquid was found for short picosecond electric pulses [5]. It should be noted that both of these extreme cases of discharge development are almost independent of the dielectric permittivity of the liquid. In contrast, nanosecond discharges may contain an important phase of electrostriction compression in the liquid that is associated with the

formation of microscopic initial voids [7]; void formation inevitably depends strongly on the dielectric permittivity of the medium and is proportional to the electrostriction pressure [7].

The same assumption was made in [8], where the authors stated that the rather weak light emission and the very small current present during the first stage of discharge suggest that the degree of ionization and, therefore, the conductivity of the channels remain rather low. The symmetry and the size of the “primary streamer” were concluded to be largely determined by the field distribution at the metallic tip [8]. The formation of micro-voids from initial nanoscale perturbations, which occur as a result of liquid-field interactions, also has been considered, e.g., in [9, 10]. It has been indicated that liquids become phase unstable, such that gas channels form along electric field lines. These channels expand, first at the base, i.e., at the location of the highest field and hence the earliest formation, creating a region of lowest density; in turn, this region gives the most favorable conditions for gas ionization.

In the present work, the formation of a nanosecond discharge in liquid dielectrics with different dielectric permittivities was studied to analyze the electrostriction mechanism of initial microscopic void formation and its influence on the dynamics of discharge development.

## Experiment

The discharge gap was constructed with a point-to-plate configuration. The high-voltage electrode was made from nickel by chemical etching. The tip radius was  $R$ , approximately equal to  $5 \mu\text{m}$  [6]. The inter-electrode gap was  $1.5 \text{ mm}$ . Density gradient visualization was performed with a laser shadowgraphic system utilizing a pulse length of  $40 \text{ ns}$  and a synchronized CCD-camera. Nanosecond pulse discharge synchronization with the laser and camera was carried out using fast photodiodes (with a typical rise time  $< 2 \text{ ns}$ ) and signals from current shunts. This scheme guaranteed a synchronization accuracy between the high-voltage pulse appearance on the discharge gap and the laser pulse better than  $2 \text{ ns}$  with a typical jitter less than  $100 \text{ ps}$ . For high-voltage pulse generation, two FID generators were used. The pulse length and maximum amplitude were  $20 \text{ ns}$  at  $+12 \text{ kV}$  and  $60 \text{ ns}$  at  $+120 \text{ kV}$ . The voltage rise times on the level 10-90 were almost identical (approximately  $3 \text{ ns}$ ). The dynamics of discharge development were investigated in three different

liquids with different dielectric permittivity constants, including water, ethanol and hexane (Table 1).

Table 1

Liquid	$\epsilon$	$M$ , MV/cm	Speed of sound (m/s)	Conductivity, ( $\text{Ohm} \times \text{cm}$ )	Isothermal compressibility, MPa
Water	81	0.3	1480	$10^5-10^6$	2200
Ethanol	27	0.5	1180	$10^6-10^7$	889
n- Hexane	2	0.7	1083	$10^{12}$	633

Under pulse breakdown conditions, the breakdown voltage increases with the decrease in pulse length. The critical electric field in the nanosecond time scale can exceed  $10-20 \text{ MV/cm}$ . To estimate a critical electric field for different pulse lengths, the empirical formula was proposed [11]:

$$E_{crit} = \frac{M \cdot P^{1/8}}{t^{1/3} S^{1/10}} \quad (1)$$

where the constant  $M$  (see Table 1) depends on the liquid and has the dimensions of  $[\text{MV/cm}]$ . In this expression, the pulse length  $t$  should be substituted in  $[\mu\text{s}]$ , the pressure in  $[\text{atm}]$ , and the electrode area  $S$  in  $[\text{cm}^2]$ . The constant  $M$  is  $0.7 \text{ MV/cm}$  for hexane and transformer oil,  $0.6 \text{ MV/cm}$  for glycerol,  $0.5 \text{ MV/cm}$  for ethanol, and  $0.6 \text{ MV/cm}$  for water in the case of breakdown from the cathode or  $0.3 \text{ MV/cm}$  in the case of breakdown from the anode.

The volumetric electrostriction force acting on a dielectric fluid in a non-uniform electric field is given by [7]:

$$\vec{F} = e \delta n \vec{E} - \frac{\epsilon_0}{2} E^2 \nabla \epsilon + \frac{\epsilon_0}{2} \nabla \left( E^2 \frac{\partial \epsilon}{\partial \rho} \right) \quad (2)$$

where the first term is the force acting on free charges with density  $e \delta n$ , the second and third terms are the volumetric density of the electrostriction forces,  $\epsilon_0$  is the vacuum dielectric permittivity,  $\rho$  is the liquid density, and  $\vec{E}$  is the electric field. The second term in equation (2) is associated with the force acting on an inhomogeneous dielectric, and the third term corresponds to the electrostriction forces in a non-uniform electric field as associated with the mechanical stresses in the dielectric [7].

In water, the electrostriction forces are 40 times higher than the forces in hexane. Thus, the fluids experimentally studied had significantly different dielectric permittivity coefficients but had similar values of the critical breakdown electric field.

Even though the isothermal compressibility coefficients for selected liquids differ only slightly, the difference in the magnitude of the electrostriction forces will cause a significant difference in the gradient of the fluid density near the tip of the

electrode. Thus, in water and ethanol, one can expect the formation of a significant density increase close to the electrode's tip in addition to a simultaneous reduction in the density and the occurrence of expansion wave propagation from the high-voltage electrode in the surrounding liquid. In contrast, the density perturbations in hexane as a result of electrostriction forces should be negligible. When a high-voltage pulse ends (the pulse width was 20 ns and 60 ns in our experiments), the electrostriction force disappears and forms a compression wave propagating behind the leading expansion wave. This complex (rarefaction wave – compression wave) have a characteristic size  $L = 20 \text{ ns} \times 1480 \text{ m/s} \sim 30 \text{ }\mu\text{m}$  immediately after the electric pulse. Within a short distance from the tip, this complex should convert into a weak sonic perturbation propagating through the liquid at the speed of sound.

## Results

Use of the high-voltage pulse with a duration of 20 ns in the water-filled gap caused two possible outcomes. At low voltages, the discharge formation was not observed. The electric field value near the tip of the electrode remained high throughout the pulse duration, forming a distinct electrostriction rarefaction wave, which propagated almost symmetrically from the electrode's tip in the discharge gap (Figure 1). As the voltage was increased, the delay time of the discharge start became very short, and the discharge commenced almost immediately as the voltage was raised. The discharge development leads to a significant electric field reduction near the electrode tip and suppresses the electrostriction mechanism. Hence, under such circumstances, the electrostriction rarefaction wave is less pronounced.

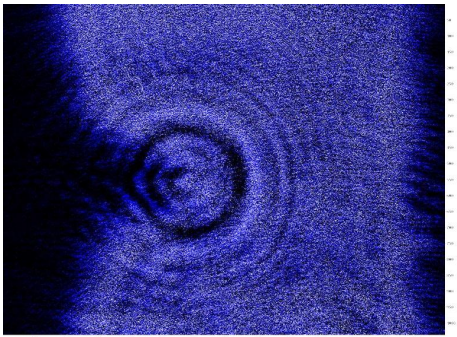


Figure 1. The electrostriction rarefaction wave without breakdown. Water,  $U = 9 \text{ kV}$ , 20 ns. The image was collected 200 ns after the HV pulse.

Simultaneously, the development of strong perturbations (shock waves) generated by energy release in the discharge can be clearly seen (Fig.2).

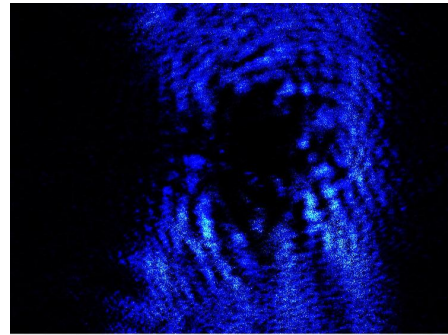


Figure 2. The streamer-leader structure formation. Water,  $U = 12 \text{ kV}$ , 20 ns. The image was collected 200 ns after the HV pulse.

In media with lower dielectric permittivity (ethanol, hexane) values, excitation by a short (20 ns) pulse did not lead to a significant fluid density decrease in the gap. The perturbations were less pronounced, arising at values below the detection threshold. A discharge phase was not observed up to a peak pulse voltage  $U \sim 12 \text{ kV}$ . In ethanol and hexane, the density distribution remained uniform for pulses of 9 kV and 12 kV each with duration of 20 ns.

For longer pulses the dynamics of the process qualitatively remained the same. In water, the pronounced hydrodynamic density perturbations resulting from the electrostriction forces were observed starting at minimal voltages (similar to Figure 1). At pulse voltages of 10 kV and higher, discharge development was observed, similar to that shown in Figure 2.

Experiments in ethanol (with 60 ns pulse duration) also showed the formation of electrostriction rarefaction waves. Similar to the discharges in water, when the voltage was increased to 25 kV, the discharge development in ethanol also reduced the magnitude of the electric field near the electrode's tip, suppressing the electrostriction forces on a large scale. Discharge in ethanol, as well as in water, led to an energy release in the channels and leads to the formation of the complex structure with multiple shock waves. The development of the initial phase of the discharge with the formation of the shock waves near the electrode tip as well as the resulting symmetrical structure of the propagating rarefaction wave takes place in the same manner. The delay in the discharge start and the relatively small energy release in the discharge at the low pulse voltage allow

to separate the initial perturbation produced by electrostriction forces and perturbations generated by the energy release in the discharge.

In hexane, the situation changed significantly. Density perturbations were not observed until the voltage reached  $U_{\text{peak}} \sim 56$  kV. When the voltage rose above this threshold, pulsed breakdown occurred with a large energy release in the discharge channel which causes the formation of strong shock waves. This behavior is fully consistent with the low value of electrostriction forces in the liquid with low dielectric permittivity. It should be noted that the observed threshold for the initiation of nanosecond discharge in hexane was more than 6 times higher than the corresponding value for water; however, in DC fields, the difference in the critical breakdown values was less than two-fold higher (Table 1).

### Discussion

Thus, the dynamics of pulsed picosecond and nanosecond discharge development in liquid water, ethanol and hexane were investigated experimentally.

Three possible mechanisms for the propagation of discharge in liquids play a different role depending on the pulse duration. The first case takes place when a "long" (microsecond) electric pulse applied in a non-conducting fluid: as a result of electrostatic repulsion, the formation of low density channels occurs. Consequently, the discharge propagates through the low-density regions. In the second case, under an "intermediate" (nanosecond) electric pulse conditions, the electrostatic forces support the expansion of nanoscale voids behind the front of the ionization wave; in the wave front the extreme electric field provides a strong negative pressure in the dielectric fluid due to the presence of electrostriction forces, forming the initial micro-voids in the continuous medium. Finally, in the third case, when a "short" (picosecond) electric pulse is utilized, the regions of reduced density cannot form because of the extremely short duration of the applied electric pulse. Ionization in the liquid phase occurs as a result of direct electron impact without undergoing a phase transition, occurring due to the acceleration of electrons by an external electric field comparable to the intramolecular fields. In this case, the discharge propagates with a velocity comparable to the local speed of light.

### References

- 1) P.Bruggeman and C.Leys. *Non-thermal plasmas in and in contact with liquids*. J. Phys. D: Appl. Phys. 42 (2009) 053001 (28pp) doi:10.1088/0022-3727/42/5/053001
- 2) Y. Yang, H. Kim, A. Starikovskiy, Y. I. Cho, A. Fridman. *Note: A Underwater Multi-channel Plasma Array for Water Sterilization*. Review of Scientific Instruments. 82, 096103 (2011); doi:10.1063/1.3633945
- 3) Yong Yang, Andrey Starikovskiy, Alexander A. Fridman, Young I. Cho. *Analysis of Streamer Propagation for Electric Breakdown in Liquid/Bioliquid*. DOI: 10.1615 Plasma Med.v1.i1.60 pages 65-83. 2010.
- 4) Y.Yang, H.Kim, A.Starikovskiy, A.Fridman, Y.I.Cho. *Application of pulsed spark discharge for calcium carbonate precipitation in hard water*. Water Research. 44 (2010) 3659-3668.
- 5) A.Starikovskiy, Y.Yang, Y.Cho, A.Fridman. *Nonequilibrium Plasma in Liquid Water - Dynamics of Generation and Quenching*. Plasma Sources Sci. Technol. 20 (2011) 024003.
- 6) I.Marinov, O.Guaitella, A.Rousseau, and S.Starikovskaia. *Successive Nanosecond Discharges in Water*. IEEE Transactions on Plasma Science, Vol. 39, No. 11, November 2011.
- 7) M.Shneider, M.Pekker and A.Fridman. *Theoretical Study of the Initial Stage of Sub-nanosecond Pulsed Breakdown in Liquid Dielectrics*. IEEE Transactions on Dielectrics and Electrical Insulation. Vol. 19, No. 5; October 2012. 1579.
- 8) W.An, K.Baumung, and H.Bluhm. *Underwater streamer propagation analyzed from detailed measurements of pressure release*. Journal of Applied Physics 101, 053302 (2007)
- 9) A.L.Kupershtokh. *Phase transitions liquid-vapor in strong electric fields*. Modern Science. Collection of Research Papers. No 2 (10). 2012. 264-271.
- 10) A.L.Kupershtokh, D.A.Medvedev. *Anisotropic instability of a dielectric liquid in a strong uniform electric field: Decay into a two-phase system of vapor filaments in a liquid*. Physical Review E, 2006, vol. 74, No. 2, p. 021505(1-5).
- 11) V.Ya.Ushakov. *Pulsed electrical breakdown in liquids*. Tomsk: Tomsk State University. 1975, 25